Atomic Spectroscopy

Article

Depth Profile Analysis of Molybdenum Disulfide Film by Glow Discharge Mass Spectrometry

Mengli Wang,[a,b] Bin Zhao,[a] Shangjun Zhuo,[b,c] Yueqin Zhu, [b,c] Lei Huang,[b,c] and Rong Qian [b,c,*]

[a] School of Material Science and Engineering, University of Shanghai for Science and Technology, 516 Jungong Road, Shanghai 200093, P.R. China

[b] National Center for Inorganic Mass Spectrometry in Shanghai, Shanghai Institute of Ceramics, Chinese Academy of Sciences, 1295 Ding Xi Road, Shanghai 200050, P.R. China

[c] Center of Materials Science and Optoelectronics Engineering, University of Chinese Academy of Sciences, 19(A) Yuquan Road, Beijing, P.R. China

Received: *February 25, 2021;* ***Revised:*** *March 19, 2021;* ***Accepted:*** *March 19, 2021;* ***Available online:*** *March 31, 2021.*

DOI: 10.46770/AS.2021.070

ABSTRACT: In this work, the depth profile analysis capability with direct current glow discharge mass spectrometry (dc-GD-MS) was evaluated by examining molybdenum disulfide (MoS_2) films on Al and steel substrates. The optimized glow discharge conditions for obtaining an ideal flat crater and an efficient signal intensity were a discharge current of 1.0–1.5 mA and a discharge pressure of 4.7 mPa. The dc-GD-MS depth profile analysis provided depth resolutions of 0.55 μm for the MoS_2/Al sample and 0.70 μm for the MoS_2/Steel sample. The interface of 4.46 μm for MoS_2/Al and 4.55 μm for MoS_2/Steel determined by dc-GD-MS was close to the thicknesses of 4.85 μm and 5.45 μm, respectively, as measured by field emission scanning electron microscopy (FE-SEM). A high-carbon steel standard sample (NIST SRM 1264a) was used to validate the reliability and accuracy of the method. Relative errors of less than 12% were obtained compared with the certified concentration and the relative standard deviation (RSD, n = 20) of typical elements within 10%. The dc-GD-MS depth profile analysis provided an efficient and reliable approach for the depth analysis of the MoS_2 film.

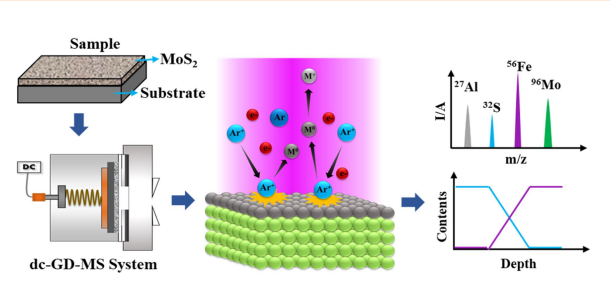

INTRODUCTION

Various thin films and coatings have been synthesized and applied into the microelectronics, space equipment and optics fields to improve the physical or mechanical properties.[1-5] Molybdenum disulfide is one of the promising films due to its chemical stability, high temperature, high pressure resistance, and high vacuum resistance.[5-6] As reported in the literature, the concentrations or distributions of trace impurities or doping elements in the films and coatings may affect the major physical or mechanical properties of the synthesized materials; therefore, it is significant to obtain detailed information on the elemental distribution or the trace impurities in films or coatings by adequate analytical techniques with the ability of high depth resolution and direct solid analysis.[8-9]

At present, many analytical techniques including secondary ion mass spectrometry (SIMS), X-ray photoelectron spectroscopy (XPS), laser ablation inductively coupled plasma mass spectrometry (LA-ICP-MS), and auger electron spectroscopy (AES) have been used for surface analysis and depth profile analysis.[10-16] Noël *et al.*[14] analyzed the depth profile of inorganic electrodes and organic layers in organic light-emitting diode stacks by TOF-SIMS. Oswald *et al.*[15] used XPS to investigate the depth distribution of Ti/Al multilayers and Ti-Al alloy layers. Detriche *et al.*[16] reported a fast approach with XPS depth profile analysis for gaining elemental distribution of the oxide layer on metal surfaces. Although these techniques are used in the depth analysis of layer materials, there are still the challenges of obtaining accurate concentration or distribution information of the elements in the depth direction without standard reference materials.

Glow discharge (GD) source coupled with mass spectrometry or optical emission spectrometry provides an alternative technique

for high resolution depth profile analysis of layered samples.[18-20] During the sputtering of the GD source, atoms are separated from the material surface layer by layer; moreover, the GD source is a very stable atomization and ionization source, and a flat crater can be obtained on the sample surface after sputtering,[7] which allows GD spectrometric techniques to efficiently determine depth profile analysis of the samples. Glow discharge mass spectrometry (GD-MS) is one of the most effective tools to directly analyze the elements of solid samples[22-28] and has been increasingly applied for the depth profile analysis of thick and thin layers.[17,21,29] The majority of the latest studies on depth profile analysis by GD-MS were performed with a time-of-flight mass spectrometer (TOF-MS).[17-18,21] Pisonero *et al.*[17] applied pulsed rf-GD-TOF-MS to measure the depth profile of B-implanted Si samples. Bouza *et al.*[29] determined the depth profile of elements in coated glasses by rf-PGD-TOF-MS. GD-MS with a double-focused magnetic sector has been successfully used for elemental determination and depth profile analysis.[9,30-31] Based on the high sputtering rates and long count integration times of the MS detector, these techniques could achieve high sensitivity and low detection limits. Di Sabatino *et al.*[30] analyzed impurities in multicrystalline *p*-type silicon samples by dc-GD-MS and obtained a depth resolution of approximately 0.5 μm. These reports have made a significant contribution to the progress of GD-MS for the direct analysis and the depth profile analysis of various samples.

For depth profile analysis, a good crater shape through the sputtering process is necessary to achieve highly resolved depth profiles.[18] The discharge conditions (such as discharge pressure, current, and voltage) should be optimized to obtain craters with a flat bottom, straight vertical sides, and no redeposition at the edges.[32-34] Previous studies have reported that the edge effect close to the crater rim possibly decreases the depth resolution of the interface.[18] Moreover, the roughness of the crater bottom increases with sputtering time, which induces a broadening of the expected profiles.[17-18,21] For evaluation of the depth profile analysis capability of GD-MS, the crater shape and depth resolution are critical parameters that need thorough investigation. Gubal *et al.*[21] obtained a flat crater by optimizing the discharge conditions and analyzed the layers of varied thicknesses (tens of nanometers to several micrometers) using a combined hollow cathode μs-dc-PGD-TOF-MS system.

In this study, dc-GD-MS was used for the depth profile analysis of MoS_2 films. The MoS_2 films were prepared by hydrothermal technology on the surface of aluminum and steel substrates. To optimize the sputtering process, the effects of discharge pressure and discharge current on the crater shape were studied. The precision of the method was verified by comparing the results with an NIST SRM sample.

EXPERIMENTAL

Materials and Sample Preparation. Aluminum and steel substrates (2 cm × 2 cm × 2 mm) were purchased from Shenzhen Rong Da Ltd. (Shenzhen, P.R. China) and used for the preparation of MoS_2/Al and MoS_2/Steel samples. Analytical grade chemical reagents, $Na_2MoO_4 \cdot 2H_2O$ and $CS(NH_2)_2$, were used in this work. A standard reference material, high-carbon steel NIST SRM 1264a, was used for validation of the dc-GD-MS system.

Molybdenum disulfide films were deposited on the aluminum and steel substrates by a hydrothermal method. First, the aluminum and steel substrates were polished with 800 grit paper and cleaned with deionized water and alcohol for 10 min and 15 min by ultrasound, respectively. For preparation of the molybdenum disulfide materials, 0.173 g $Na_2MoO_4 \cdot 2H_2O$ and 0.271 g $CS(NH_2)_2$ were placed into a beaker, 25 mL deionized water was added, and the mixture sonicated for 20 min to completely dissolve the solute particles. The solution was immediately transferred to a 35 mL reaction kettle, and the processed aluminum or steel substrate was placed in the inner tube of the reaction kettle. The sealed reaction kettle was placed in an oven and heated to 210 °C for 24 h. After the reaction kettle was cooled to room temperature, the samples were taken out, washed with deionized water and alcohol, and then dried.

Instrumentation and Conditions. The GD-MS measurement was carried out with an Auto Concept GD 90 glow discharge mass spectrometer (Mass Spectrometry Instruments Ltd., U.K.), which was equipped with a direct current power and a double-focusing Nier-Johnson magnetic sector. The GD ion source consisted of a discharge chamber and a sample holder (Fig. 1). High purity (> 99.9999%) argon gas was injected into the source chamber. The discharge cell was pre-cooled with liquid nitrogen to reduce the background noise from residual gases. During the experiments, the high intensity peaks (above 10^{-13} A) were detected using a Faraday detector, and the low intensity peaks (below 10^{-13} A) were detected with an ion counter with a Channeltron. The mass resolution was maintained at around 4000 during measurements.

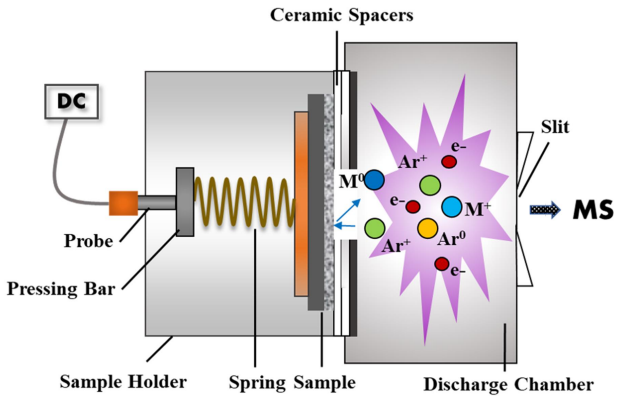

Fig. 1 Diagram of discharge chamber of dc-GD-MS.

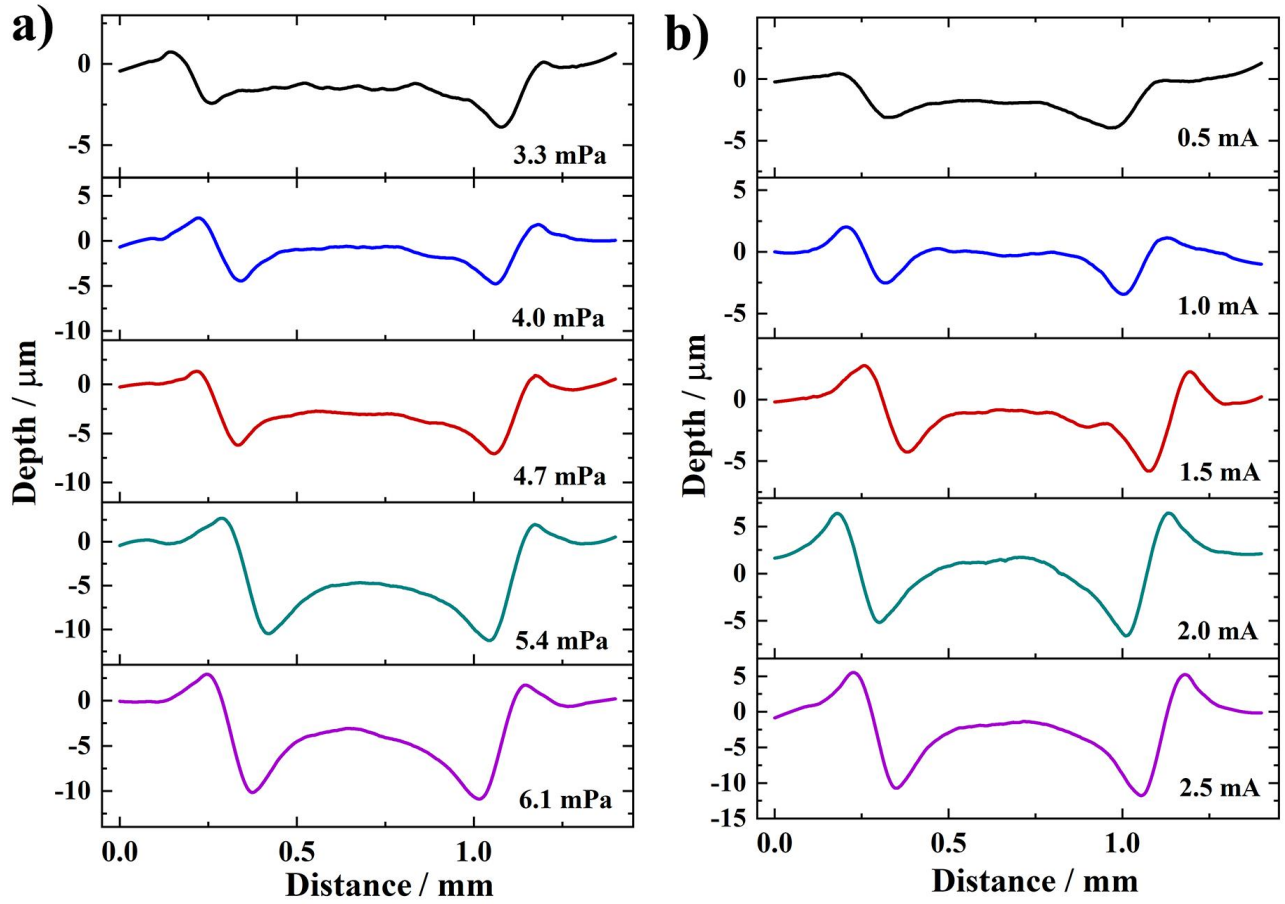

Fig. 2 Crater profile under different conditions obtained for Al substrates: (a) the discharge pressure ranged from 3.3 mPa to 6.1 mPa with a constant discharge voltage of 1.2 kV and a discharge current of 1.3 mA; (b) the discharge current ranged from 0.5 mA to 2.5 mA with a discharge voltage of 1.2 kV and a discharge pressure of 4.7 mPa.

A ceramic piece with a diameter of 10 mm was used, and the discharge voltage was fixed at 1.2 kV. The discharge current and discharge pressure were in the range of 0.5–2.5 mA and 3.3–6.1 mPa, respectively.

To study the thickness of the MoS_2 films, cross-cleavage images of the samples were investigated by field emission scanning electron microscopy (FE-SEM, SU 8220, Hitachi Ltd., Japan). Crater profiles after sputtering were determined using a surface profilometer (Dektak XT, Bruker Ltd., Germany).

RESULTS AND DISCUSSION

Optimization of experimental conditions. It has been reported that the discharge conditions in dc-GD-MS experiments may affect the sputtering and ionization in depth profile analysis. To optimize the discharge conditions, we studied the effect of the discharge pressure and discharge current on the crater shape and signal intensity using the Al substrate with a sputtering time of 40 min for each experiment. The profile and bottom roughness of the sputtered crater were measured using the Dektak XT surface profilometer.

The discharge pressure dependence of the crater profile is shown in Fig. 2a. The discharge pressure was varied between 3.3 and 6.1 mPa, the current was fixed at 1.3 mA, and the voltage was fixed at 1.2 kV. A flat crater was obtained by sputtering at low pressures (3.3–4.7 mPa); as the pressure increased (5.4–6.1 mPa), the crater profile changed to a convex shape (W-shaped crater). The W-shaped crater was induced by edge effects,[35] which negatively affected the depth profile analysis because the edge effects enhanced the argon ion flow to the aperture rim and caused inhomogeneities in the sputtering.[35-36] Fig. 3a shows that the roughness (Ra) of the crater bottom gradually increased with increasing pressure. The convex crater and high roughness of the crater bottom may adversely affect the depth analysis by reducing the depth resolution. Thus, high discharge pressure (5.4–6.1 mPa) is unfavorable for depth profile analysis.[18] Moreover, Fig. 4a shows that the signal intensity of the matrix element ^{27}Al was not sufficient for analysis at the low discharge pressure of 3.3 mPa. Thus, the discharge pressure was optimized at 4.7 mPa for subsequent experiments.

The discharge current-dependent crater profile was studied over the range of 0.5 to 2.5 mA under the optimized discharge pressure of 4.7 mPa and voltage of 1.2 kV. As shown in Fig. 2b, a flat shape of the crater was obtained at the current range of 0.5–1.5 mA. At

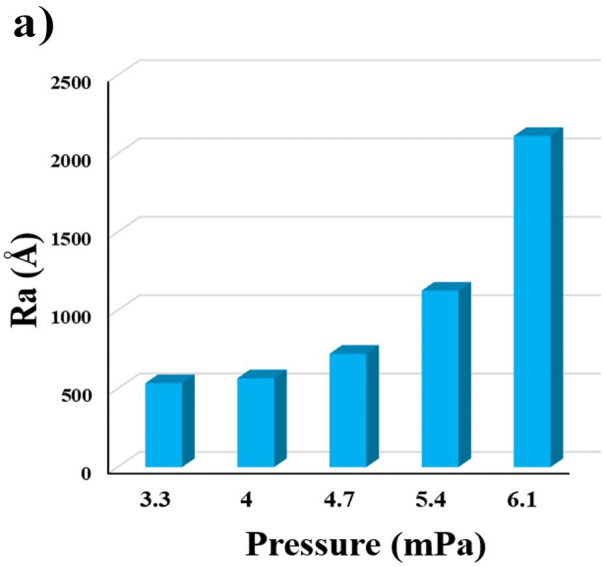

Fig. 3 Roughness (Ra) of crater bottom as an increasing trend of (a) discharge pressure and (b) discharge current at the discharge voltage of 1.2 kV.

Fig. 4 The dc-GD-MS intensity of ^{27}Al as a function of (a) discharge pressure and (b) discharge current at the discharge voltage of 1.2 kV.

high currents (2.0–2.5 mA), the edge of the crater bottom was deeper compared to the center of the crater bottom (W-shaped crater), and the roughness (Ra) of the crater bottom increased (Fig. 3b), all of which indicated that high discharge currents (2.0–2.5 mA) adversely affect the depth analysis. Moreover, Fig. 4b shows that the signal intensity was not sufficient for analysis at a low discharge current of 0.5 mA. Thus, an optimized current of 1.3 mA was considered for subsequent experiments.

Depth profile analysis of MoS_2 films. After optimization, the following experimental conditions were considered for the dc-GD-MS depth profile analysis of the MoS_2/Al and MoS_2/Steel samples: discharge voltage of 1.2 kV, discharge current of 1.3 mA, and discharge pressure of 4.7 mPa.

First, the crater features and sputtering rates of the two samples

Fig. 5 Crater profile after analysis: (a) MoS_2/Al sample and (b) MoS_2/ Steel sample.

Fig. 6 Depth profile analysis (^{32}S, ^{98}Mo, ^{27}Al and ^{56}Fe concentrations versus depth) of (a) MoS_2/Al and (b) MoS_2/Steel with discharge pressure of 4.7 mPa, discharge current of 1.3 mA and discharge voltage of 1.2 kV.

Fig. 7 SEM image of a cross-cleavage of sample: (a) MoS_2/Al and (b) MoS_2/Steel (MoS_2 film thicknesses were 4.85 μm and 5.45 μm, according to SEM measurements).

(MoS_2/Al and MoS_2/Steel) were studied after performing the dc-GD-MS experiments. As shown in Fig. 5, the crater shapes were regular, which indicated that the glow discharge was stable during the analysis. For the MoS_2/Al sample, the sputtering rate was calculated as approximately 0.16 μm·min^{-1} with a crater depth of 13 μm (Fig. 5a). For the MoS_2/Steel sample, a sputtering rate of 0.18 μm·min^{-1} with a crater depth of 14 μm was obtained by dc-GD-MS analysis.

Next, the depth profiles (^{32}S, ^{98}Mo, ^{27}Al and ^{56}Fe concentrations versus depth) of the MoS_2/Al and MoS_2/Steel samples were investigated by dc-GD-MS under optimized conditions. The concentrations were determined by the ion beam intensity ratios between the measured isotope and the matrix element. Standard relative sensitivity factors (RSFs) for the calculations were provided by the instrument manufacturer; these factors were used to convert the ion signal intensity to the mass content, and the distribution of the concentrations (^{32}S, ^{98}Mo, ^{27}Al and ^{56}Fe) versus depth was then calculated by the combination of the sputtering rate and the crater depth.[7,17] As shown in Fig. 6, the concentrations of ^{32}S and ^{98}Mo for the two samples were high at the sample surface (approximately 0–4.0 μm), and rapidly decreased with increasing depth. In contrast, the concentrations of ^{27}Al and ^{56}Fe increased sharply at depths of 4.0 μm and 3.9 μm, respectively. The results indicated that the distribution of the elemental concentrations along the depth of the MoS_2/Al and MoS_2/Steel samples can be efficiently measured by dc-GD-MS.

The MoS_2 film thicknesses for MoS_2/Al and MoS_2/Steel were estimated from the depth profile results and compared to the thicknesses measured by SEM. Fig. 7 shows the SEM images of the sample cross-cleavage, indicating a film thickness of 4.75 μm and 5.45 μm for the MoS_2/Al and MoS_2/Steel samples, respectively. The dc-GD-MS depth profile results indicated an interface depth of 4.46 μm for MoS_2/Al and 4.55 μm for MoS_2/Steel.[37-38] Thus, the thicknesses calculated for the dc-GD-MS depth profile analysis by Dektak XT surface profilometry were similar to the thicknesses measured by SEM.

Table 1. Comparison of Measured Concentration and the Certified Concentration for Elements in NIST SRM 1264a (Relative to Fe)

Elements	Measured concentration C (μg/g)	Certified concentration C_0 (μg/g)	Relative error (%)
^{55}Mn	2591.04	2500	3.64
^{28}Si	599.99	670	-10.45
^{59}Ni	1241.11	1400	-11.35
^{11}B	116.03	110	5.48
^{32}S	260.95	250	-4.38
^{96}Mo	4680.84	4900	-4.47

Finally, the depth resolution of the dc-GD-MS analysis was examined. As shown in Fig. 6, the sharp transition in the concentration curve indicates that an effective depth resolution was obtained during sputtering. Based on previous studies,[37] the depth resolution was calculated using the interface distance between 16% and 84% intensity (concentration). Depth resolutions of 0.55 μm for MoS_2/Al and 0.70 μm for MoS_2/Steel were obtained. The achieved depth resolution of 0.55 μm for the 14 μm depth crater was effective in the depth profile analysis of the MoS_2 films.[30]

Accuracy validation of the dc-GD-MS technique. In the current work, the analytical accuracy of dc-GD-MS was evaluated using high-carbon steel NIST SRM 1264a (elements uniformly distributed with depth). The experiment was performed with the optimized discharge parameters of 1.2 kV, 1.3 mA and 4.7 mPa.

The relative standard deviation (RSD, n = 20) of the concentrations of ^{55}Mn, ^{28}Si, ^{59}Ni, ^{11}B, ^{32}S and ^{96}Mo in NIST SRM 1264a was less than 10%, which indicated that the discharge and the sputtering of the sample were stable during dc-GD-MS analysis. Table 1 shows the measured concentrations and certified concentrations of ^{55}Mn, ^{28}Si, ^{59}Ni, ^{11}B, ^{32}S and ^{96}Mo in NIST SRM 1264a; the relative errors were all within 12%, which demonstrated that dc-GD-MS is an accurate method for elemental analysis.

CONCLUSIONS

In this work, the capability of dc-GD-MS for depth profile analysis was evaluated by determining the elemental distribution along the depth of MoS_2 films. Depth profile analysis of MoS_2/Al and MoS_2/Steel samples was performed, and depth resolutions of 0.55 μm and 0.70 μm, respectively, were obtained. The accuracy of the dc-GD-MS technique was validated by determining typical elements in NIST SRM 1264a; the relative errors of the typical elements were calculated within 12%, and the relative standard deviation (RSD, n = 20) of the concentrations was less than 10%. The results show that the dc-GD-MS system is a prospective and accurate technique for the efficient analysis of materials.

AUTHOR INFORMATION

Corresponding Author

*R. Qian

Email address: qianrong@mail.sic.ac.cn

Notes

The authors declare no competing financial interest.

ACKNOWLEDGMENTS

The authors acknowledge the financial support of the National Natural Science Foundation of China (No. 21775156), Shanghai Intergovernmental International Cooperation Project (No. 19520712000), Shanghai Science and Technology Innovation Action Project (No. 20142201100), and the Shanghai Technical Platform of Testing on Inorganic Materials (No. 19DZ2290700).

REFERENCES

1. H. Tan, P. Babal, M. Zeman, and A. H. M. Smets, *Sol. Energy Mater. Sol. Cells*, 2015, **132**, 597-605. https://doi.org/10.1016/j.solmat.2014.10.020
2. E. W. Brooman, *Part I, Met. Finish.*, 2000, **98**, 42-50. https://doi.org/10.1016/S0026-0576(00)81602-5
3. N. Aizawa, Y. J. Pu, M. Watanabe, T. Chiba, K. Ideta, N. Toyota, M. Igarashi, Y. Suzuri, H. Sasabe, and J. Kido, *Nat. Commun.*, 2014, **5**, 5756. https://doi.org/10.1038/ncomms6756
4. S. Choi, D. S. Jung, and J. W. Choi, *Nano. Lett.*, 2014, **14**, 7120-7125. https://doi.org/10.1021/nl503620z
5. G. Colasetal, A. Saulot, E. Regis, and Y. Berthier, *Wear*, 2015, **330**, 448-460. https://doi.org/10.1016/j.wear.2015.01.011
6. Y. Q. Xing, Z. Wu, J. J. Yang, X. S. Wang, and L. Liu, *Surf. Coat. Tech.*, 2020, **385**, 125396. https://doi.org/10.1016/j.surfcoat.2020.125396
7. I. T. Spitsberg and K. Putyera, *Surf. Coat. Tech.*, 2001, **139**, 35-43. https://doi.org/10.1016/S0257-8972(00)01162-2
8. T. Kodalle, D. Greiner, V. Brackmann, K. Prietzel, A. Scheu, T. Bertram, P. Reyes-Figueroa, T. Unold, D. Abou-Ras, R. Schlatmann, C. A. Kaufmann, and V. Hoffmann, *J. Anal. At. Spectrom.*, 2019, **34**, 1233-1241. https://doi.org/10.1039/C9JA00075E
9. J. Pisonero, N. Bordel, C. G. Vega, B. Fernández, R. Pereiro, and A. Sanz-Medel, *Anal. Bioanal. Chem.*, 2013, **405**, 5655-5662. https://doi.org/10.1007/s00216-013-6914-1
10. V. Možná, J. Pisonero, M. Holá, V. Kanický, and D. Günther, *J. Anal. At. Spectrom.*, 2006, **21**, 1194-1201. https://doi.org/10.1039/B606988F
11. D. Abou-Ras, R. Caballero, C.-H. Fischer, C.A. Kaufmann, I. Lauermann, R. Mainz, et al., *Microsc. Microanal.* 2011, **17**, 728-751. https://doi.org/10.1017/S1431927611000523
12. J. S. Jang, H. H. Hwang, H. J. Kang, H. C. Chae, Y. D. Chung, and K. J. Kim. *Appl. Surf. Sci.*, 2013, **282**, 777-781. https://doi.org/10.1016/j.apsusc.2013.06.052

13. M. A. Reshchikov, M. Vorobiov, O. Andrieiev, K. Ding, N. Izyumskaya, V. Avrutin, A. Usikov, H. Helava, and Y. Makarov, *Sci. Rep.*, 2020, **10**, 2223. https://doi.org/10.1038/s41598-020-59033-z
14. C. Noël, N. Tuccitto, Y. Busby, M. Auer-Berger, A. Licciardello, E. J. W. List-Kratochvil, and L. Houssiau, *ACS Appl. Polym. Mater*., 2019, **1**, 1821-1828. https://doi.org/10.1021/acsapm.9b00292
15. S. Oswald, E. Lattner, and M. Seifert, *Surf. Interface Anal*., 2020, **52**, 924-928. https://doi.org/10.1002/sia.6820
16. S. Detriche, S. Vivegnis, J. F. Vanhumbeeck, A. Felten, P. Louette, F.U. Renner, J. Delhalle, and Z. Mekhalif, *J. Electron. Spectros.*, 2020, **243**, 146970. https://doi.org/10.1016/j.elspec.2020.146970
17. J. Pisonero, L. Lobo, A. Tempez, A. Bensaola, N. Badi, and A. Sanz-Medel, *Sol. Energy Mater. Sol. Cells*, 2010, **94**, 1352-1357. https://doi.org/10.1016/j.solmat.2010.04.002
18. L. Lobo, B. Fernández, and R. Pereiro, *J. Anal. At. Spectrom.*, 2017, **32**, 920-930. https://doi.org/10.1039/C7JA00055C
19. B. Fernandez, L. Lobo, P.Tyagi, V. Stoichkov, J. Kettle, and R. Pereiro, *Talanta*, 2019, **192**, 317-324. https://doi.org/10.1016/j.talanta.2018.09.059
20. C. J. Rao, S. Ningshen, and J. Philip, *Spectrochim. Acta Part B.*, 2020, **172**, 105973. https://doi.org/10.1016/j.sab.2020.105973
21. A. Gubal, V. Chuchina, Y. Lyalkin, V. Mikhailovskii, V. Yakobson, N. Solovyev, and A. Ganeev, *J. Anal. At. Spectrom.*, 2020, **35**, 1587-1596. https://doi.org/10.1039/D0JA00088D
22. C. Gonzalez-Gago, P. Smid, T. Hofmann, C. Venzago, V. Hoffmann, and W. Gruner, *Anal. Bioanal. Chem.* 2014, **406**, 7473-7482. https://doi.org/10.1007/s00216-014-8186-9
23. B. Fernandez, L. Lobo, P. Tyagi, V. Stoichkov, J. Kettle, and R. Pereiro, *Talanta* 2019, **192**, 317-324. https://doi.org/10.1016/j.talanta.2018.09.059
24. J. Pisonero, I. Feldmann, N. Bordel, A. Sanz-Medel, and N. Jakubowski, *Anal. Bioanal. Chem.* 2005, **382**, 1965-1974. https://doi.org/10.1007/s00216-005-3357-3
25. B. Siqin, R. Qian, S. J. Zhuo, J. Gao, J. Jin, and Z. Y. Wen, *J. Anal. At. Spectrom.* 2014, **29**, 2064-2071. https://doi.org/10.1039/C4JA00172A
26. W. Schelles and R. E. Van Grieken, *Anal. Chem.* 1996, **68**, 3570–3574. https://doi.org/10.1021/ac960441u
27. R. Qian, S. J. Zhuo, Z. Wang, and P. K. Robinson, *J. Anal. At. Spectrom.* 2013, **28**, 1061-1067. https://doi.org/10.1039/C3JA50029B
28. J. Dong, R. Qian, W. Xiong, H. Qu, B. Siqin, S. Zhuo, J. Jin, Z. Wen, and P. He, *Int. J. Mass Spectrom.* 2014, **361**, 1-8. https://doi.org/10.1016/j.ijms.2014.01.018
29. M. Bouza, B. Fernández, R. Pereiro, N. Bordel, and A. Sanz-Medel, *J. Anal. At. Spectrom.*, 2015, **30**, 1108-1116. https://doi.org/10.1039/C4JA00474D
30. M. Di Sabatino, C. Mondanese, and L. Arnberg, *J. Anal. At. Spectrom.*, 2014, **29**, 2072-2077. https://doi.org/10.1039/C4JA00175C
31. R. Matschat, J. Hinrichs, and H. Kipphardt, *Anal. Bioanal. Chem.*, 2006, **386**, 125-141. https://doi.org/10.1007/s00216-006-0645-5
32. L. A. Heras, O.L. Actis-Dato, M. Betti, E.H. Toscano, U. Tocci, R. Fuoco, and S. Giannarelli, *Microchem. J.*, 2000, **67**, 333-336. https://doi.org/10.1016/S0026-265X(00)00083-7
33. R. E. Galindo, E. Forniés and J. M. Albella, *J. Anal. At. Spectrom.*, 2005, **20**, 1108-1115. https://doi.org/10.1039/B502771C
34. G. Paudel, S. Khromov, M. Kasik, H. J. Roven, and M. D. Sabatino, *J. Anal. At. Spectrom.*, 2020, **35**, 1450-1457. https://doi.org/10.1039/D0JA00055H
35. A. Bogaerts and R. Gijbels, *Spectrochim. Acta Part B.*, 1997, **52**, 765-777. https://doi.org/10.1016/S0584-8547(96)01623-0
36. A. Bogaerts and R. Gijbels, *J. Anal. At. Spectrom.*, 1998, **13**, 945-953. https://doi.org/10.1039/A800329G
37. G. H. Morrison, K. L. Cheng, and M. Grasserbauer, *Pure Appl. Chem.*, 1979, **51**, 2243-2250. https://doi.org/10.1351/pac197951112243
38. S. Hofmann, *Appl. Phys.*, 1976, **9**, 59-66. https://doi.org/10.1007/BF00901910